Optimal Placement of Precast Bridge Deck Slabs with respect to Precast Girders using LiDAR

S.H. Yoon[a], Q. Wang[a,b] and H. Sohn[a]

[a]Department of Civil and Environmental Engineering,
Korea Advanced Institute of Science and Technology, South Korea
[b]Department of Civil and Environmental Engineering,
The Hong Kong University of Science and Technology, Hong Kong
E-mail: sh.yoon@kaist.ac.kr, qwangau@ust.hk, hoonsohn@kaist.ac.kr

Abstract –

Many bridges have been constructed using precast components because they offer faster production, lower cost, and more efficient construction compared to conventional in-situ construction. For coupled behavior of bridges slabs and girders, shear pockets on the deck slabs and shear connectors on the girders need to be properly connected. However, precast girders can be easily deformed once they are placed on sites because of their heavy weights, time dependent effects of creep and shrinkage, pre or post tensioning, etc. Once the girders are deformed, shear pockets and shear connectors may no longer match properly. This study proposes a technique which can automatically identify mismatches between shear connectors and shear pockets using LiDAR and identify the optimal placement of precast deck slabs with respect to precast bridge connectors. First, precast bridge deck slabs and precast girders are scanned using a LiDAR. Then, unnecessary noise data are removed using a DBSCAN-based algorithm. Afterwards, the dimensional features such as locations and sizes of shear pockets and shear connectors are estimated from the point cloud data, respectively. Finally, the optimal placement of deck slabs is identified to minimize the mismatches between shear pockets and shear connectors using the Levenberg-Marquardt (LM) method. To validate the effectiveness of the proposed technique, an experiment was conducted on a real precast girder. The experimental results demonstrate that the proposed technique can effectively and efficiently estimate the optimal placement of deck slabs with respect to precast girders.

Keywords –

LiDAR; Precast girder; Precast bridge deck slab; Precast bridge connector; Optimal placement

1 Introduction

Precast bridges are constructed by connecting precast components, such as precast girders and precast bridge deck slabs, on construction sites. For coupled behavior of precast bridge deck slabs and precast girders, the shear pockets on the deck slabs and the shear connectors on the girders need to be properly connected [1]. However, three reasons may lead to the mismatch between the shear pockets and the shear connectors including (1) dimensional errors of precast girders and deck slabs occurred in fabrication process, (2) deformation of precast girders due to their weights, time dependent creep and shrinkage, and pre or post tensioning [2], and (3) incorrect orientation and location of shear connectors. Therefore, it is of great significance to identify the optimal placement of precast bridge deck slabs with respect to precast girders to minimize the mismatches between shear pockets and shear connectors. However, precast components are currently manually inspected by certified inspectors using traditional tools such as measuring tapes, which is time-consuming, expensive, and subjective [3]. Hence, it is necessary to develop techniques that can automatically and accurately assess the dimensional quality of precast components such as precast bridge deck slabs and precast girders for estimating the optimal placement of precast bridge deck slabs.

This study proposes an automated optimal placement estimation technique for precast bridge deck slabs with respect to precast girders using LiDAR. After obtaining scan data using LiDAR, the proposed technique firstly removes noise components using a DBSCAN-based algorithm. Then, a RANSAC-based plane detection algorithm is used to extract scan data associated with shear connectors. Next, a two-class classification algorithm is applied to extract scan data which only belong to shear connector heads. Afterwards, the orientation and location of each shear connector are

estimated. Finally, the optimal placement of precast bridge deck slabs is estimated by solving a nonlinear minimization problem based on the previously estimated orientation and location of shear connectors and the shear pocket location obtained in a previous study [4]. This paper is organized as follows. Section 2 provides the research background on precast bridge construction and LiDAR. The developed optimal placement estimation technique for precast bridge deck slabs are described in Section 3. Section 4 validates the proposed technique using a field experiment. Finally, Section 5 provides a summary and conclusions of this study.

2 Research background

2.1 Precast bridge connections

For the safety and serviceability of precast bridges, it is critical to ensure a tight connection between precast bridge deck slabs and precast girders [1]. The deck slabs and the girders are connected by the shear pockets on the deck slabs and the shear connectors on the girders. A shear pocket is usually a rectangular hole throughout a precast bridge deck slab as shown in Figure 1 (a). On the other hand, a stud type shear connector, which is the type of shear connectors considered in this study, is a steel rod welded on the top flange of a precast girder and is composed of a connector head and a connector body as shown in Figure 1 (b). Multiple shear connectors are placed inside a single shear pocket as shown in Figure 1 (c), and the gap is filled by cement for coupled behavior. The main function of the coupled shear pockets and shear connecters is to prevent vertical separation of precast bridge deck slabs from precast girders and to minimize longitudinal movement between the deck slabs and the girders [5]. From time to time, shear pockets and shear connectors are mismatched due to dimensional errors of precast bridge deck slabs and precast girders, time dependent deformations of precast girders, and faulty shear connectors to name a few. However, such mismatches are hardly discovered until precast bridge deck slabs are actually placed on precast girders, resulting in construction delay and cost overrun. Therefore, it is necessary to identify the foreseeable mismatches at the fabrication stage of precast components.

2.2 Light Detection And Ranging (LiDAR)

LiDAR measures the distance to a target by illuminating the target with laser beams and analyzing the reflected signals. Due to the rapid rotation of the scanner head in both horizontal and vertical directions, a laser scanner can measure the distances at different directions at a high speed within a region of interest (ROI). The obtained scanned points called 'point cloud data' consist of three-dimensional X, Y, and Z coordinates of each scan point with respect to the scanner.

The distance can be measured by two different principles, time-of-flight and phase-shift. The time-of-flight system measures the round trip time between the emitted light pulse and the returned pulse. Since the velocity of the laser pulse is known, the distance can be derived from the round trip time. On the other hand, the phase-shift system emits an amplitude modulated continuous wave and estimates the distance by measuring the phase difference between the emitted and reflected waves. The time-of-flight system is usually adopted for a long range measurement while the phase-shift system is adopted for a short distance sensing with a higher accuracy [6].

Although LiDAR has been used for the quality assessment of precast deck slabs [7,8,9,10], no study has been conducted on the quality assessment of precast girders or the optimal placement of precast deck slabs.

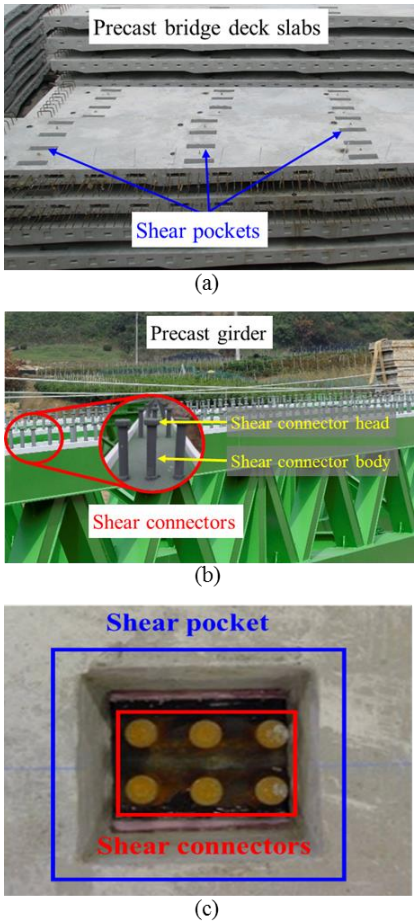

Figure 1. Coupling between shear pockets and shear connectors. (a) Precast bridge deck slabs

with shear pockets. (b)Precast girders with shear connectors. (c) A connection between shear pockets and shear connectors.

3 Optimal placement of precast bridge deck slabs with respect to precast girders

This Section illustrates the developed technique for estimating the optimal placement of precast bridge deck slabs. Before the optimal placement estimation, the dimensions of precast bridge deck slabs and precast girders are assessed, which are illustrated in Sections 3.1 and 3.2, respectively. Afterwards, based on the dimension estimation, the optimal placement of precast bridge deck slabs is estimated with respect to precast girders by minimizing mismatches between shear pockets on the deck slabs and shear connectors on the girders, which is illustrated in Section 3.3.

3.1 Dimension estimation of precast bridge deck slabs

The dimensions of precast bridge deck slabs are assessed during fabrication in the precast concrete factory. The technique developed in the authors' previous study [11] is used, which has the following four steps. Firstly, the scan data of precast bridge deck slabs are acquired using LiDAR. Then, coordinate transformation and noise data removal are undertaken. Thirdly, key dimensional features, i.e. edges and corners of shear pockets, are extracted from the scan data. Finally, the dimensional properties of the shear pockets are computed from the extracted corners.

3.2 Dimension estimation of precast girders

The dimensions of precast girders are estimated at the construction site since deformations can occur after they are placed on site. LiDAR is located on a crane to acquire the scan data of the target girder. The acquired scan data are processed through four steps to estimate the dimensions of precast girder, (1) data preprocessing, (2) shear connector identification, (3) shear connector head extraction, and (4) estimation of shear connector orientation and location, as follows.

3.2.1 Data preprocessing

This step aims to remove noise data from raw scan data of precast girders and align the coordinates of the scan data with respect to the local coordinates of the precast girders. Scan data usually contain three categories of data including valid points, background points, and mixed pixels, as shown in Figure 2. A mixed pixel occurs when the laser beam is split by edges of target objects and can be located anywhere along the line of the laser beam [12]. Both mixed pixels and background points are considered as noise data and need to be removed.

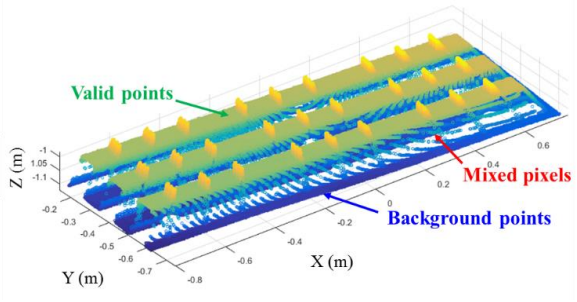

Figure 2. Three categories of scan data: valid points, background points, and mixed pixels.

Compared to valid points and background points, mixed pixels have larger distances to their neighbors, resulting in a lower spatial density. Thus, a DBSCAN-based data classification algorithm developed by Wang et al. [13] is applied for data classification. This DBSCAN-based algorithm performs classification based on spatial densities such that mixed pixels are classified as noise data due to low density while valid points and background points become two clusters. Furthermore, valid points are distinguished from background points as they have shorter distances to the LiDAR. After noise removal, valid points representing the as-built object (the precast girder) are remained.

Once the as-built object is extracted, the 3D coordinates of the as-built object are transformed into a new Cartesian coordinate system so that the as-built object best matches the as-design object. The same coordinate transformation method as used in the previous study [14] is applied to the as-built object as follows. (1) Extract the fitted planes of the as-built and as-design objects. (2) Transform the as-built object so that the two fitted planes are overlapped. (3) Find the transformation that minimizes the root mean square distances (RMSD) between the as-built and as-design object boundaries by iterative search. (4) Transform the as-built object with the previously obtained transformation to match the as-design object.

3.2.2 Shear connector identification

A precast girder mainly consists of two parts, a girder plane and shear connectors. This step aims to distinguish the girder plane and shear connectors, and extract shear connectors from the scan data. The girder plane and the shear connectors are distinguished using a plane extraction algorithm, namely Random Sample Consensus (RANSAC) [15]. The girder plane is estimated using RANSAC with a reference vector of [0

0 1], as shown in Figure 3 (a). To implement RANSAC, three parameters (*S*, *N*, and δ) are decided as follows. (1) The number of random selection (*S*) should be set such that the mathematical model can be estimated. Since a plane is extracted from the scan data, *S* is set as three. (2) The maximum number of random trials (*N*) is determined based on a probabilistic approach. The probability (*P*) that at least one out of *N* random trials can successfully select three scan points belonging to the girder plane is represented as follows:

$$P = 1 - (1 - \alpha^3)^N \quad (1)$$

where α is the ratio between the number of girder plane data and the number of the total scan data. The ratio α is estimated as the ratio between the girder plane area and the total girder area and approximately equals to 0.90, and *P* is set as 0.999. Hence, *N* is set as six according to Equation (2).

$$N = \frac{\log(1 - 0.999)}{\log(1 - 0.90^3)} \approx 5.29 \quad (2)$$

(3) The tolerance (δ) refers to the maximum orthogonal distance from an inlier to the plane. Since girders require cambering in order to compensate for dead load deflections, δ is set as 1.2 × maximum camber, where 1.2 is a safety factor. Given the above three parameters, the girder plane is estimated using RANSAC. Scan data which do not belong to the estimated girder plane are regarded and extracted as shear connectors, as shown in Figure 3 (b).

3.2.3 Shear connector head extraction

The extracted shear connector data contain three parts including (1) shear connector heads, (2) shear connector bodies, and (3) noise data. Due to the LiDAR position, some parts of shear connector bodies are occluded by their own shear connector heads. Therefore, only the shear connector heads are extracted in this study, using the K-means clustering method [16].

To partition the shear connector heads from the other scan data, three features are selected for K-means clustering as follows. Firstly, the neighboring scan points of each scan point within a radius of 2 cm are extracted (Figure 4 (a)). Then, the eigenvalues ($\lambda_1 \geq \lambda_2 \geq \lambda_3 \geq 0$) of the covariance matrix of its neighbors are calculated [17]. Based on these eigenvalues, two geometric features, namely planarity and variance, are defined and calculated as $((\lambda_2 - \lambda_3) / \lambda_1)$ and $(\lambda_1 / \lambda_1 + \lambda_2 + \lambda_3)$, respectively. Furthermore, a third geometric feature, namely average height, is defined and calculated as the average height of neighboring scan points. As shown in Figure 4 (b), shear connector heads, shear connector bodies, and noise data have substantially different values for these three geometric features. Using the three features, K-means clustering algorithm is applied to extract the shear connector heads.

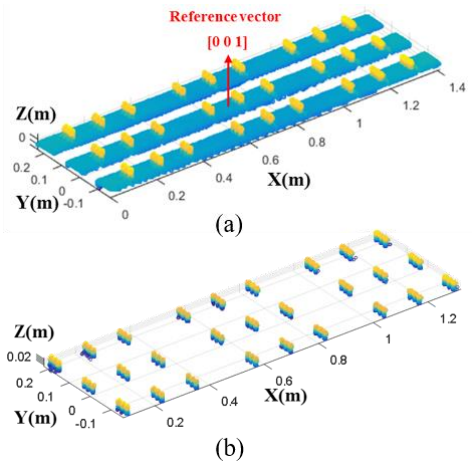

Figure 3. Identification of shear connectors using RANSAC. (a) Scan data of the as-built precast girder. (b) Identified shear connectors.

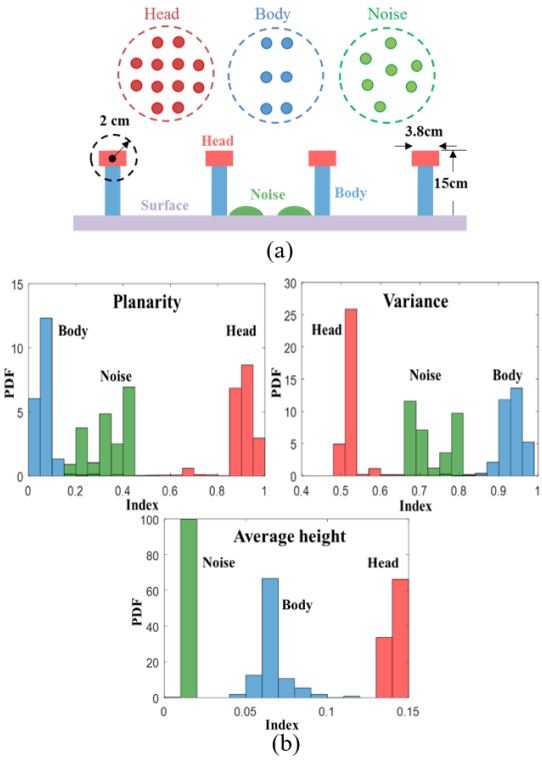

Figure 4. Shear connector heads extraction using K-means clustering. (a) Neighboring points of three types of scan points. (b) Values of geometric features for three types of scan points.

3.2.4 Estimation of shear connector orientation and location

The center position of each shear connector head is

computed as the mean value of all the scan points located on the shear connector head and considered as the location of the shear connector head (L_Head). Afterwards, the orientation (θ) of each shear connector is estimated by calculating the angle between the normal vector of each shear connector head and a reference vector [0 0 1] using dot production, as illustrated in Figure 5 (a).

$$\theta = \cos^{-1}\left(\frac{n_1 \cdot n_2}{\|n_1\|\|n_2\|}\right) \quad (3)$$

where n_1 and n_2 are the normal vector of shear connector head and the reference vector at the center position of L_Head, respectively. The position of each shear connector on the girder plane (L) is estimated based on the L_Head, θ, and the length of the shear connector body provided from the as-design model, as shown in Figure 5 (b).

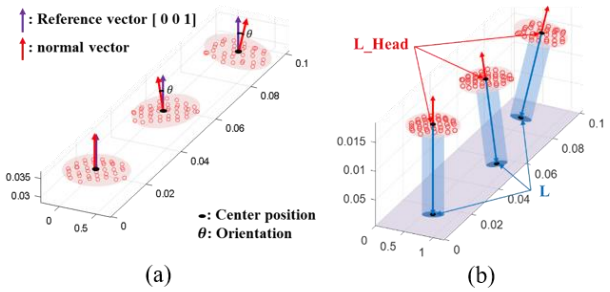

Figure 5. Orientation and location estimation of shear connector. (a) Estimation of L_Head and orientation (θ) of the shear connector head. (b) Estimation of the shear connector position (L).

3.3 Optimal placement of precast bridge deck slabs

The optimal placement of as-built precast bridge deck slabs suggests the location of each deck slab with respect to the deformed as-built precast girders such that mismatches between shear pockets and shear connectors can be minimized. First, three terminologies are defined before proceeding to the optimal placement estimation: *integrated deck slab*, *bundle area* (S_i), and *inner area* (A_i), as illustrated in Figure 6. All the precast bridge deck slabs that will be placed within a single span is defined as one *integrated deck slab* as shown in Figure 6 (a). Then, S_i is defined by the following three steps: (1) All the shear connectors that are supposed to be placed within a single shear pocket are identified; (2) the location and the area of each shear connector's head and body (red and blue circles in Figure 6 (b)) are estimated based on L_Head, L, and as-design diameters of the shear connector's head and body; (3) A rectangular area including all the areas of the shear connector's heads and bodies is defined as S_i. Finally, the fraction of S_i that falls within the shear pocket, is defined as A_i (Figure 6 (c)). The optimal placement is estimated through two steps, (1) coarse matching, and (2) fine matching, as described below.

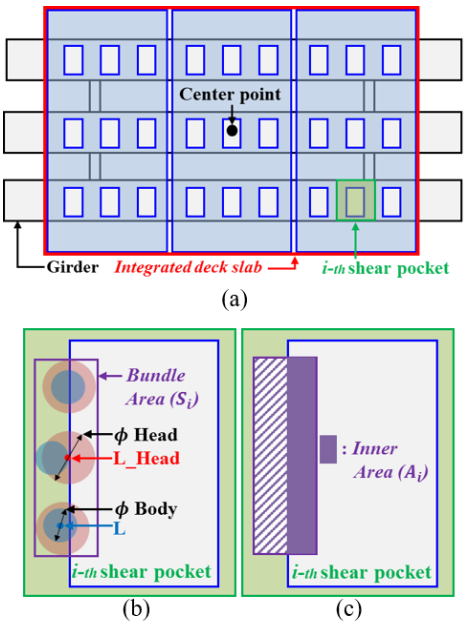

Figure 6. Fundamental concepts for the optimal placement estimation. (a) *Integrated deck slab*. (b) *Bundle area* (S_i), and (c) *inner area* (A_i).

3.3.1 Coarse matching

In the coarse matching step, an integrated deck slab is shifted by an initial translation vector T_0 so that its center point aligns with the center point of the precast girder. Then, all the *inner areas* within the integrated deck slab are calculated and their summation (ΣA_i) is computed. Next, the integrated deck slab is shifted again to maximize ΣA_i. If all the bundle of shear connectors are placed inside the boundaries of the shear pocket where they are supposed to be in, ΣA_i is maximized and becomes equal to the summation of all *bundle areas* (ΣS_i). Hence, the optimal placement estimation becomes the problem of minimizing the squared sum of the discrepancies between S_i and A_i as follows.

$$\mathbf{T}^c = \underset{\mathbf{T}^c}{\operatorname{argmin}} \sum_{i=1}^{n} (S_i - A_i)^2 \quad (4)$$

where n is the number of shear pockets within the *integrated deck slab* and $\mathbf{T}^c = [T_x^c, T_y^c]^T$, where T_x^c and T_y^c are the coarse translation values of the *integrated deck slab* in X and Y axes, respectively. This

nonlinear optimization problem is solved using the Levenberg-Marquardt (LM) method [18]. S_i and A_i at the *i-th* shear pocket are obtained by Equations (5) and (6), respectively.

$$S_i = \left(a_{x,i}^2 - a_{x,i}^1\right) \times \left(a_{y,i}^2 - a_{y,i}^1\right) \tag{5}$$

$$A_i = \left[\min\left(c_{x,i}^2, a_{x,i}^2\right) - \max\left(c_{x,i}^1, a_{x,i}^1\right)\right] \times \left[\min\left(c_{y,i}^2, a_{y,i}^2\right) - \max\left(c_{y,i}^1, a_{y,i}^1\right)\right] \tag{6}$$

where $a_{x,i}^1$, $a_{x,i}^2$, $a_{y,i}^1$, and $a_{y,i}^2$ are the X and Y coordinates of corner points of *i-th bundle area* as shown in Figure 7 and $c_{x,i}^1$, $c_{x,i}^2$, $c_{y,i}^1$, and $c_{y,i}^2$ are the X and Y coordinates of the four corner points of the coarsely translated i-th shear pocket and are determined by the translation vector $\mathbf{T}^c$ as follows (Figure 7).

$$c_{x,i}^1 = b_{x,i}^1 + T_x^c,\ c_{x,i}^2 = b_{x,i}^2 + T_x^c$$
$$c_{y,i}^1 = b_{y,i}^1 + T_y^c,\ c_{y,i}^2 = b_{y,i}^2 + T_y^c \tag{7}$$

where $b_{x,i}^1$, $b_{x,i}^2$, $b_{y,i}^1$, and $b_{y,i}^2$ are the X and Y coordinates of the four corner points of the *i-th* as-design shear pocket location in X and Y axes, respectively, (Figure 7). The translation vector $\mathbf{T}^c$ is iteratively estimated by solving the nonlinear minimization problem described in Equation 4.

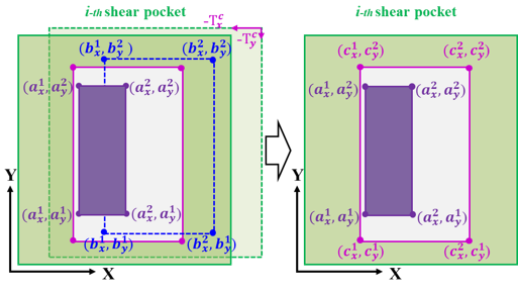

Figure 7. Change of the overlap area between the *bundle area* (S_i) and the *inner area* (A_i) after coarse matching by $\mathbf{T}^c$.

3.3.2 Fine matching

Once the integrated deck slab is shifted as a whole, now each deck slab within the integrated deck slab is individually shifted for fine matching. Fine matching starts with the deck slab which has the largest number of remaining mismatches. Then, fine matching operates on the next slab with the second largest number of mismatches, and repeats until all the mismatches disappear or until the last slab is shifted. For the *k-th* deck slab, the fine translation vector is found as follows.

$$\mathbf{T}_k^F = \underset{\mathbf{T}_k^F}{argmin} \sum_{j=1}^{m} (S_j - A_j)^2 \tag{8}$$

where $\mathbf{T}_k^F$ is the fine translation vector of the *k-th* deck slab, and m is the number of shear pockets within the *k-th* deck slab. Note that there are the maximum allowable horizontal and vertical relative movements between two adjacent deck slabs, denoted as σ_x and σ_y in Figure 8, respectively. Therefore, the values of $\mathbf{T}_{k,x}^F$ and $\mathbf{T}_{k,y}^F$ in $\mathbf{T}_k^F$ are limited within the range of $[-\sigma_x/2, \sigma_x/2]$ and $[-\sigma_y/2, \sigma_y/2]$, respectively. Similar to Eq. (4), this optimization problem is again solved using the LM method. After coarse matching and fine matching, the total translation vector $\mathbf{T}_k$ of the k-*th* deck slab becomes:

$$\mathbf{T}_k = \mathbf{T}_0 + \mathbf{T}^c + \mathbf{T}_k^F \tag{9}$$

Finally, any remaining mismatched shear connectors are visualized in Figure 8 so that they can be adjusted or repaired if necessary.

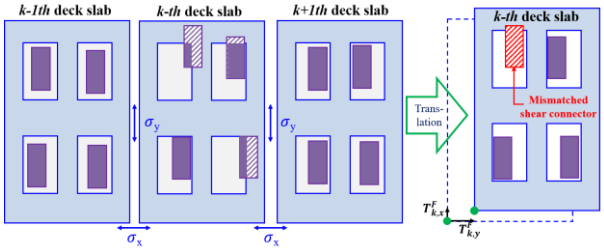

Figure 8. Fine matching of the *k-th* deck slab and visualization of the mismatched shear connector.

4 Field experiment

4.1 Experimental set-up

To validate the proposed technique for optimal placement estimation of precast bridge deck slabs, a field test was conducted on a real precast bridge girder. The field test was conducted at a precast concrete factory located in Jincheon-gun, Republic of Korea. Scan data of the precast girder were acquired using a FARO Focus 3D laser scanner, as shown in Figure 9 (a). The precast girder had dimensions of 13,100 mm × 3,200 mm × 1,503 mm with 234 shear connectors as shown in Figure 9 (b). Each shear connector had a height, head diameter, and body diameter of 150 mm, 38 mm, and 25 mm, respectively. The scan distance from the precast girder to the laser scanner was 13 m. Due to the large scale of the precast girder and the long scan distance, the highest angular resolution, i.e., 0.009°, was selected. The data acquisition and data processing

took about 20 minutes and 30 minutes on average, respectively. As described in Section 3.1, the dimensions of the deck slabs were estimated using the technique developed in Kim et al. [11], and the developed dimensions estimation technique was applied for the girders.

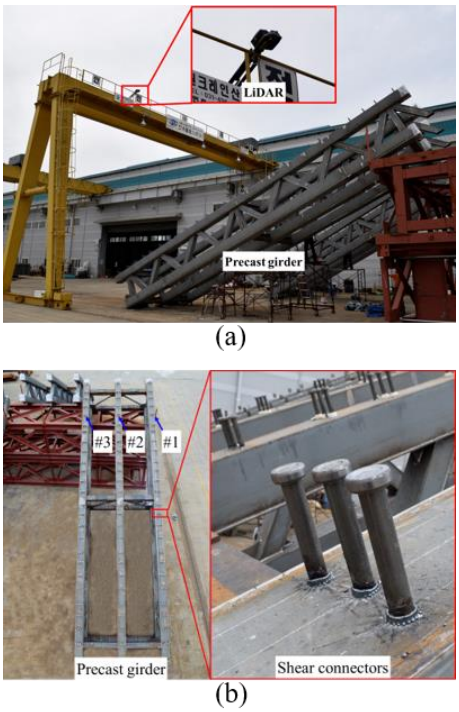

Figure 9. Test configuration of the full-scale girder scanning. (a) Test set-up, (b) A full-scale precast girder.

4.2 Experimental results for optimal placement estimation

The proposed optimal placement estimation technique was applied to the precast girder used in the experiment. When the deck slabs were placed based on the as-design placement, there were a total 54 mismatches between the shear pockets and shear connectors, as shown in Figure 10 (a). After the proposed coarse matching step, the number of mismatches was reduced to 4, as shown in Figure 10 (b). Finally, all the mismatches were eliminated after the fine matching step, as shown in Figure 10 (c). The amount of horizontal and vertical translations for the optimal placement of all the six deck slabs were presented in Table 1.

Table 1 The amount of horizontal and vertical translations of all the six deck slabs for optimal deck slab placement.

Translation (mm)	X axis	Y axis	X axis	Y axis	X axis	Y axis
Slab No.	#1		#2		#3	
Coarse	26.5	-25.0	26.5	-25.0	26.5	-25.0
Fine	0	4.6	0	2.9	0	-3.9
Total	26.5	-20.4	26.5	-22.1	26.5	-28.9
Slab No.	#4		#5		#6	
Coarse	26.5	-25.0	26.5	-25.0	26.5	-25.0
Fine	0	-5.9	0	0	0	0
Total	26.5	-30.9	26.5	-25.0	26.5	-25.0

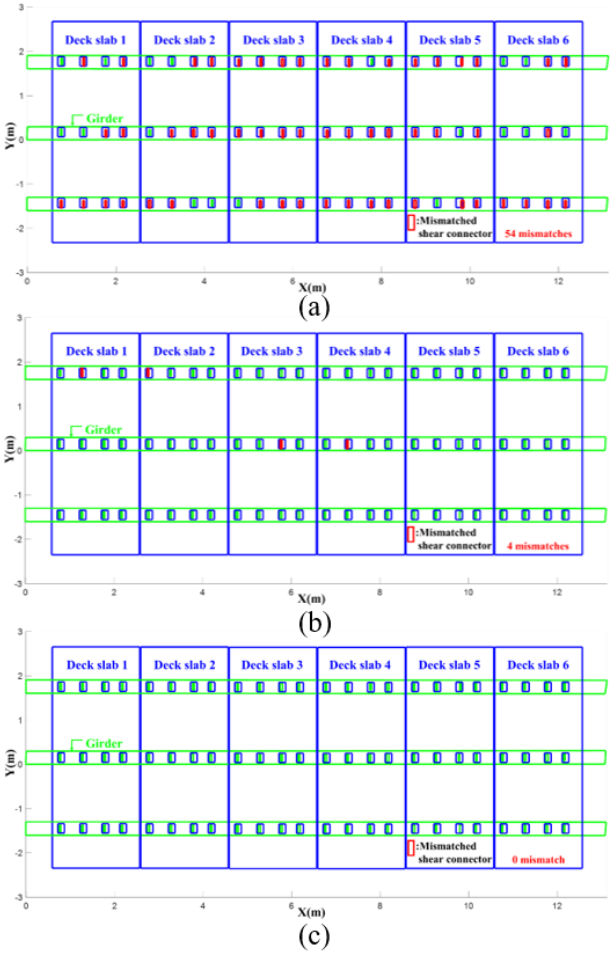

Figure 10. Result of optimal placement. (a) As-design placement. (b) Coarse matching. (c) Fine matching.

5 Conclusions

This study presents an optimal placement estimation technique for precast bridge deck slabs with respect to

precast girders to minimize mismatches between the shear pockets on the deck slabs and the shear connectors on the girders using LiDAR. The scan data from a girder are acquired using LiDAR and processed through five steps, (1) data preprocessing, (2) shear connector identification, (3) shear connector head extraction, (4) estimation of shear connector orientation and location, and (5) optimal placement estimation. The proposed technique was validated through a full-scale precast girder experiment at an actual construction site. During the optimal placement estimation, 54 mismatches were reduced to 4 mismatches after coarse matching, and no mismatch existed after fine matching.

One major limitation of this study is that LiDAR must be located on the top of precast girders to acquire laser scan data. However, it can be sometimes difficult to impossible to place the LiDAR in actual construction sites. One possible solution is to mount the LiDAR on an unmanned aerial vehicle (UAV) for scanning.

Acknowledgement

This research was supported by a grant (13SCIPA01) from Smart Civil Infrastructure Research Program funded by Ministry of Land, Infrastructure and Transport (MOLIT) of Korea Government and Korea Agency for Infrastructure Technology Advancement (KAIA).

References

[1] M.A. Issa, T.A Patton, H.A. Abdalla, A.A. YOUSIF, and M.A. Issa, Composite behavior of shear connections in full-depth precast concrete bridge deck panels on steel stringers, PCI journal, 48(5):76-89, 2003.

[2] K.A. Byle, N.H. Burns, and R.L. Carrasquillo, Time-dependent deformation behavior of prestressed high performance concrete bridge beams, *Work*, 580(6), 1997.

[3] B.M. Phares, G.A. Washer, D.D. Rolander, B.A. Graybeal, and M. Moore, Routine highway bridge inspection condition documentation accuracy and reliability, *Journal of Bridge Engineering*, 9(4):403-413, 2004.

[4] M.-K. Kim, H. Sohn, and C.-C. Chang, Automated dimensional quality assessment of precast concrete panels using terrestrial laser scanning, *Automation in Construction*, 45:163-177, 2014.

[5] J. Qureshi, D. Lam, and J. Ye, Effect of shear connector spacing and layout on the shear connector capacity in composite beams, *Journal of Constructional Steel Research*, 67(4):706-719, 2011.

[6] J. Shan, and C.K. Toth, Terrestrial laser scanners, Topographic laser ranging and scanning: principles and processing, *CRC press*, 2008.

[7] M.-K. Kim, H. Sohn, and C.-C. Chang, Localization and quantification of concrete spalling defects using terrestrial laser scanning, *Journal of Computing in Civil Engineering*, 29(6), 2014.

[8] M-K Kim, J.C. Cheng, H Sohn, and C.-C. Chang, A framework for dimensional and surface quality assessment of precast concrete elements using BIM and 3D laser scanning, *Automation in Construction*, 49:225-238, 2015

[9] Q. Wang, M-K Kim, H Sohn, and J.C. Cheng, Surface flatness and distortion inspection of precast concrete elements using laser scanning technology, *Smart Structures and Systems*, 18(3):601-623, 2016.

[10] Q. Wang, H Sohn, and J.C. Cheng, Development of a mixed pixel filter for improved dimension estimation using AMCW laser scanner, *Journal of Photogrammetry and Remote Sensing*, 119:246-258, 2016.

[11] M.-K. Kim, Q. Wang, J.-W. Park, J.C. Cheng, H. Sohn, and C.-C. Chang, Automated dimensional quality assurance of full-scale precast concrete elements using laser scanning and BIM, *Automation in Construction*, 72:102-114, 2016.

[12] M. Hebert, and E. Krotkov, 3D measurements from imaging laser radars: how good are they?, *Image and Vision Computing*, 10(3):170-178, 1992.

[13] A.A. Siddiqui, A New Inspection Method Based on RGB-D Profiling, *Virginia Tech*, 2015.

[14] Q. Wang, M.-K. Kim, J.C. Cheng, and H. Sohn, Automated quality assessment of precast concrete elements with geometry irregularities using terrestrial laser scanning, *Automation in Construction*, 68:170-182, 2016.

[15] M.A. Fischler, and R.C. Bolles, Random sample consensus: a paradigm for model fitting with applications to image analysis and automated cartography, *Communications of the ACM*, 24(6):381-395, 1981.

[16] S. Lloyd, Least squares quantization in PCM, *IEEE transactions on information theory*, 28(2):129-137, 1982.

[17] R. Blomley, M. Weinmann, J. Leitloff, and B. Jutzi, Shape distribution features for point cloud analysis-a geometric histogram approach on multiple scales, ISPRS Annals of the Photogrammetry, *Remote Sensing and Spatial Information Sciences*, 2(3):9, 2014.

[18] D.W. Marquardt, An algorithm for least-squares estimation of nonlinear parameters, *Journal of the society for Industrial and Applied Mathematics*, 11(2):431-441, 1963.